JOURNAL OF AGRICULTURAL AND FOOD CHEMISTRY

Article

pubs.acs.org/JAFC

Intestinal Metabolism of Two A-type Procyanidins Using the Pig Cecum Model: Detailed Structure Elucidation of Unknown Catabolites with Fourier Transform Mass Spectrometry (FTMS)

Anna Engemann,[†,‡] Florian Hübner,[‡] Sebastian Rzeppa,[‡] and Hans-Ulrich Humpf*[,†,‡]

[†]NRW Graduate School of Chemistry, Westfälische Wilhelms-Universität Münster, Wilhelm-Klemm-Strasse 10, 48149 Münster, Germany

[‡]Institut für Lebensmittelchemie, Westfälische-Wilhelms Universität Münster, Corrensstrasse 45, 48149 Münster, Germany

Supporting Information

ABSTRACT: Procyanidins, as important secondary plant metabolites in fruits, berries, and beverages such as cacao and tea, are supposed to have positive health impacts, although their bioavailability is yet not clear. One important aspect for bioavailability is intestinal metabolism. The investigation of the microbial catabolism of A-type procyanidins is of great importance due to their more complex structure in comparison to B-type procyanidins. A-type procyanidins exhibit an additional ether linkage between the flavan-3-ol monomers. In this study two A-type procyanidins, procyanidin A2 and cinnamtannin B1, were incubated in the pig cecum model to mimic the degradation caused by the microbiota. Both A-type procyanidins were degraded by the microbiota. Procyanidin A2 as a dimer was degraded by about 80% and cinnamtannin B1 as a trimer by about 40% within 8 h of incubation. Hydroxylated phenolic compounds were quantified as degradation products. In addition, two yet unknown catabolites were identified, and the structures were elucidated by Fourier transform mass spectrometry.

KEYWORDS: *procyanidin A2, cinnamtannin B1, microbial catabolites, pig cecum, bioavailability, structure elucidation, FTMS, intestinal metabolism, quinone methide pathway (QM), retro-Diels-Alder fission (RDA), heterocyclic ring fission (HRF)*

INTRODUCTION

In several studies procyanidins as oligomers and polymers of flavan-3-ols were confirmed to have positive health impacts such as anticancer and antioxidant activities.[1−4] Because of their occurrence as the second most abundant natural phenolic compounds after lignin, procyanidins are frequently found in foodstuffs such as fruits, berries, beans, nuts, cocoa, and wine.[5] In cranberries, 6.9 mg/100 g fresh weight procyanidin A2 (**1**) and 2.1 mg/100 g fresh weight cinnamtannin B1 (**2**) can be found.[6] Other food samples containing procyanidin A2 (**1**) and cinnamtannin B1 (**2**) are, for example, apricots, blueberries, litchi, pears, red plum, and cinnamon.[5,6] For systemic health effects, it is important to know the bioavailability. Substances that are not degraded or absorbed during the passage of the stomach and small bowel reach the large bowel. Here they underlie the catabolic potential of the microbiota. A high stability of procyanidins under gastric and duodenal digestion conditions in vitro has been shown,[7] and also the stability under gastric conditions has been proven in vivo after the consumption of a cacao beverage.[8] In contrast to the found stability, Kahle and co-workers found a pH-dependent degradation or hydrolysis of procyanidin B2 under simulated duodenal and gastric conditions.[9] Appeldoorn and co-workers observed no absorption of procyanidin B2 and A-type procyanidin trimers and only little absorption for procyanidins A1 and A2, which was only 5−10% of the absorption rate of the monomers in studies with in situ perfusion models using rats.[10] They suggested that an increasing polymerization rate decreased the absorption during passage through the gastrointestinal tract. Therefore, procyanidins reach the large bowel either intact or partially degraded by pH effects. In the large bowel they underlie degradation by the microbiota. The bacterial catabolites that are formed might also be bioavailable and therefore responsible for positive health impacts, for example, cardioprotective effects.[5] In addition, hydroxyphenylacetic acids have been suggested to inhibit platelet aggregation.[11] In conclusion, procyanidins, especially those with higher polymerization rates, reach the large bowel, where they can be degraded by the microbiota. The amount of degradation and the formed catabolites are important to estimate possible health impacts caused by these substances.

With its high density of catabolically active bacteria, which can contain a mixture of more than 400 different species, the pig cecum model simulates the in vivo situation well. All preparatory steps in the model are done under anaerobic conditions. A fecal suspension is prepared with a reductive phosphate buffer containing sodium sulfide.[12−14] Furthermore, studies using fluorescence in situ hybridization (FISH) revealed that the composition of the pig cecum microbiota is similar to the human microbiota for most bacterial species.[13]

In previous studies it has been shown that flavan-3-ols (catechin, epicatechin, their glucosides, and B-type procyanidins) are degraded by the microbiota to hydroxylated phenylcarboxylic acids (**4**−**12**) and phloroglucinol (**3**).[15−17] The dimeric procyanidins B2 and B5 were degraded to different

Received: September 27, 2011
Revised: November 29, 2011
Accepted: December 16, 2011
Published: December 16, 2011

degrees in the pig cecum model. Within 2 h 62 ± 36% of procyanidin B5 were degraded. In contrast to this, procyanidin B2 was nearly totally degraded within 4 h. Both procyanidins were degraded with large interindividual differences concerning the incubation with pig cecal inocula.[18] Stoupi et al. found several unknown catabolites after incubation experiments of procyanidin B2 with isolated human fecal microbiota. These catabolites had monomeric as well as dimeric character as was shown by mass spectrometric measurements.[19] After incubation with pig inoculal suspension, the structure of one monomeric catabolite of procyanidin B2 was identified by the accurate mass and its fragmentation pattern by van't Slot.[18]

In this study, the microbial catabolism of two A-type procyanidins was investigated in the pig cecum model, namely, procyanidin A2 (**1**) and cinnamtannin B1 (**2**) (Figure 1). A-type procyanidins have an additional ether linkage between the C2 of the upper unit and the C7 or C5 of the lower unit.[5] Much information concerning the microbial degradation of B-type procyanidins is available in the literature, but information about the catabolism of A-type procyanidins is still lacking. Therefore, the intestinal metabolism of two A-type procyanidins was studied.

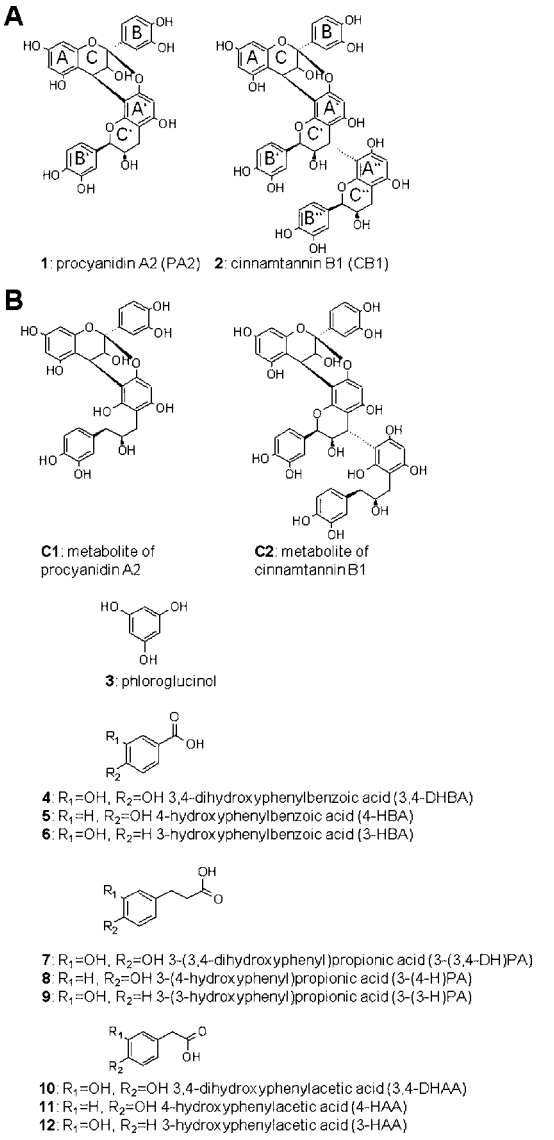

Figure 1. Structures of (A) the incubated procyanidins (procyanidin A2 (**1**) and cinnamtannin B1 (**2**)) and (B) phenolic compounds (**3**–**12**) and new procyanidin catabolites **C1** and **C2** as intestinal degradation products.

MATERIALS AND METHODS

Chemicals and Reagents. 4-Hydroxyphenylbenzoic acid (4-HBA) (**5**), 3-hydroxyphenylbenzoic acid (3-HBA) (**6**), phloroglucinol (**3**), 3-(3,4-dihydroxyphenyl)propionic acid (3-(3,4-DH)PA) (**7**), 3-hydroxyphenylacetic acid (3-HAA) (**12**), and dry pyridine were obtained from Merck (Darmstadt, Germany). 3-(4-Hydroxyphenyl)-propionic acid (3-(4-H)PA) (**8**), 3,4-dihydroxyphenylacetic acid (3,4-DHAA) (**10**), and 4-hydroxyphenylacetic acid (4-HAA) (**11**) were purchased from Sigma-Aldrich (Steinheim, Germany). 3-(3-Hydroxyphenyl)propionic acid (3-(3-H)PA) (**9**) was provided by ABCR (Karlsruhe, Germany). 3,4-Dihydroxyphenylbenzoic acid (3,4-DHBA) (**4**) and syringic acid were obtained from Roth (Karlsruhe, Germany). Quercetin was provided from Extrasynthese (Genay, France). All chemicals were purchased in p.A. quality.

Procyanidin A2 (**1**) and cinnamtannin B1 (**2**) were isolated from litchi pericarp (*Litchi chinensis*). Therefore, plant material was ground and extracted with acetone/water (70:30, v/v). The acetone was removed, and the aqueous residue was extracted with ethyl acetate. The ethyl acetate extract was reduced to dryness. The residue was dissolved in a small amount of ethanol and loaded on a column filled with Sephadex LH20 (GE Healthcare, München, Germany). Elution was performed with ethanol as eluent and monitored by UV detection and thin-layer chromatography on silica with ethyl acetate/formic acid/water (90:5:5, v/v/v) as mobile phase. For detection vanillin/hydrochloric acid spray reagent was used. On the basis of the results the fractions were combined. A further purification of the fraction containing procyanidin A2 (**1**) was not necessary. The fraction containing cinnamtannin B1 (**2**) was purified by column chromatography (25 × 390 mm) on MCI CHP20P (Sigma-Aldrich): Chromatographic separation was performed by using the following binary gradient of water/methanol (80:20, v/v) (A) and water/methanol (20:80, v/v) (B) at a flow rate of 6 mL/min: 0% B (0 min), 0% B (60 min), 50% B (240 min), 50% B (300 min).

The purity of the isolated procyanidins was investigated by RP-HPLC coupled to a diode array (DAD), fluorescence (FLD), and evaporative light scattering (ELSD) detector. The system consisted of a DGU-20A3 degasser, two LC-20AT pumps, an SIL-20A autosampler, a SPD-M20A DAD, a RF-10AXL FLD, and an ELSD-LT ELSD (all from Shimadzu, Duisburg, Germany). The separation was performed on a LiChrospher RP18 column, 250 × 2 mm, with 5 μm particle size (Merck) as stationary phase. The mobile phase consisted of the following linear gradient of water/formic acid (99.9:0.1 v/v) (A) and acetonitrile (B): 10% B (0 min), 10% B (5 min), 15% B (15 min), 40% B (30 min). The flow rate was set to 300 μL/min. The injection volume was 10 μL (dissolved in 0.1% formic acid/acetonitrile 10:90, v/v). In the case of diode array detection absorbance was recorded at 280 nm. The excitation wavelength of the FLD was 276 nm, and the emission was monitored at 316 nm. The ELSD parameters were the following: temperature, 40 °C; and pressure, 2.5 bar (air). The purity of procyanidin A2 is >97.7% and that of cinnamtannin B1 >96.8%.

The identity of standard substances was checked by mass spectrometry and nuclear resonance spectroscopy. The data are in accordance with the literature.[20−23] Stereochemistry was investigated by circular dichroism spectroscopy and is also in agreement with literature data.[23]

Solvents for HPLC as well as other chemicals were purchased from Merck or Sigma-Aldrich in gradient or reagent grade quality. Water was purified with a Milli-Q Gradient A10 system (Millipore, Schwalbach, Germany).

Sample Preparation and Analysis. *Preparation of Inoculum.* Ceca obtained from freshly slaughtered pigs (German Landrace or Angler Sattel × Pietrain) bred under biodynamic conditions were used exclusively. The pigs were 10−12 months old and weighed between

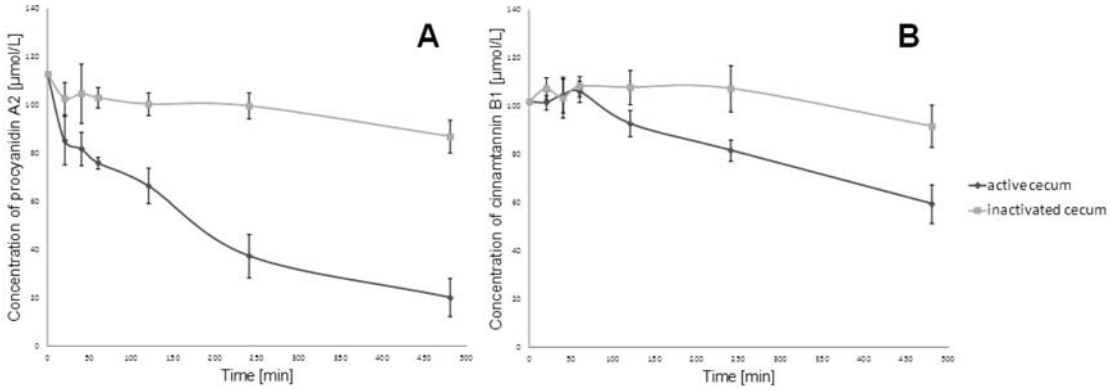

Figure 2. Degradation curve of procyanidin A2 (**1**) (A) and cinnamtannin B1 (**2**) (B) in pig cecal inocula (100 μM procyanidin A2 or cinnamtannin B1 was incubated) (n = 6, mean ± SD).

120 and 150 kg. The ceca were obtained during slaughtering, and, after removal with ligation to maintain anaerobic conditions, stored in an anaerobic jar containing Anaerocult A (Merck) for transport. In the laboratory the ceca were used directly without further storage. The time of storage was intended to be as short as possible and was alike for all ceca. All preparation steps were done in an anaerobic chamber under strict anaerobic conditions. In addition, all buffers, solutions, and glass vessels were flushed with a mixture of N_2 and CO_2 (5/1; v/v) before use to achieve total exclusion of oxygen. Sixty grams of the isolated inocula of each cecum was diluted with 60 mL of 0.15 M PBS (pH 6.2) containing a trace element solution 0.0125% (13.2 g/100 mL $CaCl_2{\cdot}2H_2O$, 10.0 g/100 mL $MnCl_2{\cdot}4H_2O$, 1.0 g/100 mL $CoCl_2{\cdot}6H_2O$, and 8.0 g/100 mL $FeCl_3{\cdot}6H_2O$) and an 11.1% Na_2S solution (575.9 mg/100 mL of 0.037 M NaOH).[12] Larger particles of the fecal solution were removed by filtration through net lace, and the solution was used for incubation experiments. In addition, an inactivated fecal suspension was prepared after sterilization of an aliquot of the feces at 121 °C for 15 min at 1.1 bar using an AMB240 autoclave (Astell, Kent, U.K.). Each incubation experiment was performed with three different ceca and for each cecum in duplicate. The metabolic activity of each cecum was tested by incubation with quercetin as control substance (data not shown).

Incubation Experiments. Stock solutions of procyanidin A2 (**1**) and cinnamtannin B1 (**2**) (1 mM in methanol) were diluted 1:10 (v/v) with the active or inactivated fecal solution. For each incubation 900 μL of fecal suspension was used. In addition, blank samples were prepared by diluting methanol 1:10 (v/v) with fecal suspension. Incubation took place for 20 min up to 8 h at 37 °C under continuous shaking. The catabolism of the bacteria was stopped after incubation by deep-freezing at −80 °C.

HPLC-FLD Analysis. Procyanidin A2 (**1**) and cinnamtannin B1 (**2**) were extracted after quick defrosting of the fecal suspension at 37 °C with 0.5 mL of 1% hydrochloric acid in methanol (v/v). After 15 min of sonication and centrifugation at 12000*g* for 10 min, the supernatant was removed. The pellet was extracted with 0.5 mL of 1% hydrochloric acid in methanol, sonicated for 15 min, and centrifuged at 12000*g* for 10 min. The supernatants were combined and again centrifuged at 12000*g* for 10 min. An aliquot of the supernatant was analyzed by HPLC with fluorescence detection (FP-2020 Plus fluorescence detector, Jasco, Groß-Umstadt, Germany; excitation wavelength, 276 nm; emission wavelength, 316 nm). For chromatographic separation a binary gradient delivered by a PU-2085 Plus pump and a LG-2080-02S gradient unit (Jasco) of methanol (A) and 0.1% formic acid in water (B) with a flow rate of 400 μL (0.0 min 5% A, 15.5 min 100% A, 15.6 min 5% A, 21.0 min 5% A) was used. The column used was a 150 mm × 2 mm i.d., 5 μm, Nucleodur C18 isis (Macherey-Nagel, Dueren, Germany), which was heated at 30 °C by a CO-2060 Plus column thermostat (Jasco). Five microliters of the solution was injected using an XLC 3159AS autosampler (Jasco). Concentrations were calculated using an external calibration curve ranging from 5 to 100 μM with a linear regression of R^2 = 0.9945 for procyanidin A2 (**1**) and R^2 = 0.9990 for cinnamtannin B1 (**2**). The data were processed using Jasco ChromPass version 1.8.6.1. The recovery was analyzed by spiking inactivated fecal suspensions with 100 μM procyanidin A2 (**1**) and cinnamtannin B1 (**2**) and following the extraction procedure mentioned above. The recoveries were 113% for procyanidin A2 (**1**) and 102% for cinnamtannin B1 (**2**). In addition, the samples were screened at 280 and 360 nm by a multiwavelength detector (DAD) MD-2010 Plus (Jasco) for catabolites.

GC-MS Analysis. Hydroxylated phenolic compounds were analyzed by gas chromatography coupled with a mass specific detector (GC-MS) (7980 A gas chromatograph, 5975C mass specific detector, Agilent Technologies, Santa Clara, CA). For analysis, 420 μL of the procyanidin extract, also used for HPLC analysis, and syringic acid as internal standard (IS) with a final concentration of 20 μM were evaporated using a vacuum concentrator BA-VC 300 H (H. Saur, Reutlingen, Germany) at 40 °C and 20 mbar. The dried sample was derivatized with 150 μL of *N*,*O*-bis(trimethylsilyl)acetamide (BSA) for 30 min at 55 °C and afterward diluted with 150 μL of dry pyridine. The chromatographic separation took place on an HP5-MS column (30 m × 0.25 mm × 0.25 μm; Agilent Technologies) with the following temperature program: 50 °C was held for 1 min and then the temperature was raised by 5 °C/min until 120 °C, which was held for 10 min and then increased by 20 °C/min until 320 °C. The final temperature was held for 4 min. One microliter was injected using the splitless mode at 320 °C by MPS2Xl Twister autosampler (Gerstel, Mülheim, Germany). The mass spectrometer was used in the electron impact mode (EI) at 70 eV with a source temperature of 230 °C and a quadrupole temperature of 150 °C. Mass spectra were obtained in the full scan mode from m/z 50 to 800. Data were processed using Chemstation software (Agilent), version E.02.00493. Concentrations of the phenolic degradation products were calculated using calibration curves ranging from 3 to 50 μM.

Fourier Transform Mass Spectrometry (FTMS). For mass spectrometric measurements either the solution for FLD measurements was used directly for syringe pump experiments or the unknown catabolites were isolated after HPLC analysis by collecting the catabolite and evaporating the eluent. The acid of the HPLC eluate was removed by solid phase extraction on Strata C18-E columns (55 μm, 70 A, 200 mg/3 mL). The C18 cartridges were washed with 3 mL of water and the unknown metabolites eluted with 6 mL of methanol. FTMS was performed on an LTQ Orbitrap XL using heated electrospray ionization (HESI) (Thermo Fisher Scientific, Bremen, Germany). Negative ionization was used for the detection of the procyanidins and their catabolites. The measurements were either done directly with a syringe pump or after chromatographic separation using the same stationary phase as for FLD measurements. Source conditions were as follows for syringe pump experiments: spray voltage, 3.2 kV; vaporizer temperature, 50 °C; capillary temperature, 275 °C (procyanidin A2)/225 °C (cinnamtannin B1); sheath gas, 8 arb (procyanidin A2)/7 arb (cinnamtannin B1); auxiliary gas, 5 arb; capillary voltage, −27 V (procyanidin A2)/−40 V (cinnamtannin B1);

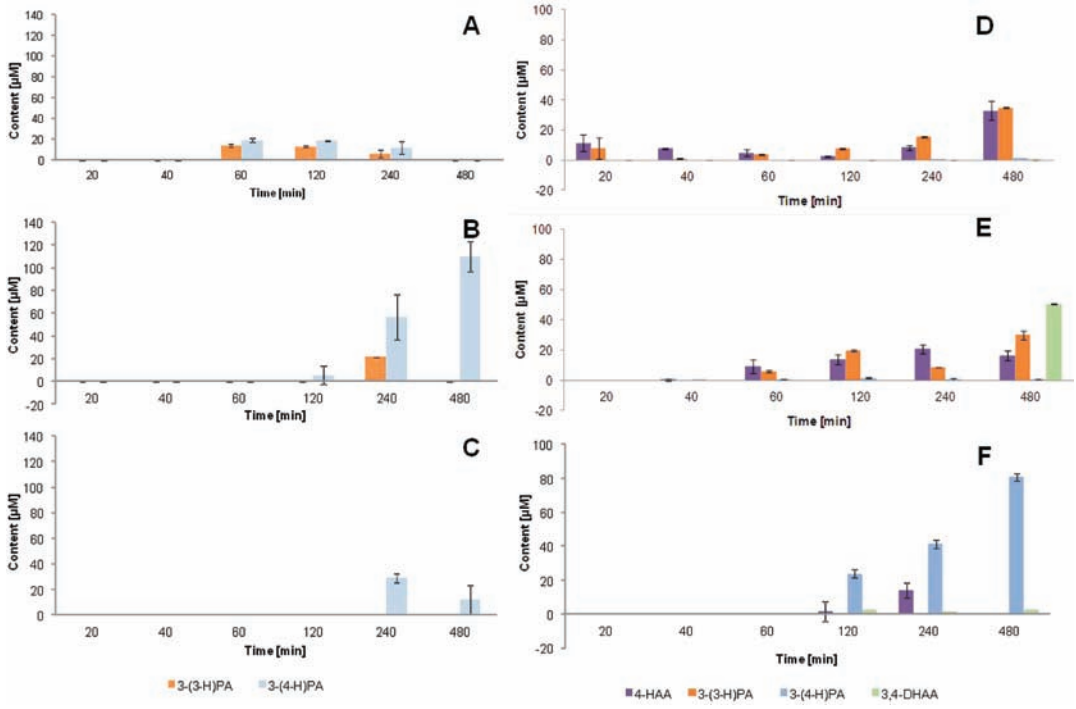

Figure 3. Contentration profiles of phenolic compounds 3-(4-hydroxyphenyl)propionic acid (3-(4-H)PA, **8**), 3-(3-hydroxyphenyl)propionic acid (3-(3-H)PA, **9**), 3,4-dihydroxyphenylacetic acid (3,4-DHAA, **10**), and 4-hydroxyphenylacetic acid (4-HAA, **11**). Compounds **8** and **9** are the main degradation products of procyanidin A2 (**1**) for cecum 1 (A), cecum 2 (B), and cecum 3 (C) and **8**−**11** the main catabolites of cinnamtannin B1 (**2**) for cecum 1 (D), cecum 2 (E), and cecum 3 (F) (n = 6, mean ± SD).

tube lens voltage, −120 V (procyanidin A2)/−124 V (cinnamtannin B1). Source conditions were as follows for HPLC experiments: spray voltage, 3.2 kV; vaporizer temperature, 250 °C; capillary temperature, 275 °C (procyanidin A2)/225 °C (cinnamtannin B1); sheath gas, 40 arb; auxiliary gas, 20 arb; capillary voltage, −34 V (procyanidin A2)/−40 V (cinnamtannin B1); tube lens voltage, −114 V (procyanidin A2)/−124 V (cinnamtannin B1). Resolution was set to 30000 or 60000. Data were processed using Xcalibur software (Thermo Fisher Scientific), version 2.0.7.

RESULTS AND DISCUSSION

Degradation of Procyanidins and Formation of Hydroxylated Phenolic Compounds. Two A-type procyanidins, procyanidin A2 (**1**) and cinnamtannin B1 (**2**), were incubated with porcine microbiota. Both procyanidins were metabolized by the intestinal bacteria. After 8 h of incubation, about 80% of procyanidin A2 (**1**) and about 40% of cinnamtannin B1 (**2**) (Figure 2) were degraded, which is in agreement with literature data. Dimers such as procyanidin B2 are degraded more quickly in comparison to trimers.[18] As typical bacterial catabolites after C-ring cleavage small phenolic degradation products **3**−**10** were identified after degradation of procyanidin A2 (**1**) with **8** and **9** as the main catabolites and **3**−**12** after degradation of cinnamtannin B1 (**2**) with **8**, **9**, **10**, and **11** as the main catabolites (see Figure 1 for structures). Due to the complexity of the degradation products Figure 3 shows only the main catabolites. The concentration profiles of all degradation products can be found in the Supporting Information (Figures S1 and S2). The liberation of the different hydroxylated phenolic compounds showed large interindividual differences concerning the quality and quantity (see Figure 3). For procyanidin A2 (**1**) the main catabolite is **8** in all three incubated ceca (Figure 3A−C). In cecum 1 (Figure 3A) the maximum of **8** is reached after 60 min of incubation with 19 μM. In cecum 2 (Figure 3B) the highest content is reached after 8 h of incubation time with 109 μM. Here, **8** seems to be accumulated and about 50% of procyanidin A2 (**1**) is catabolized to **8**. In cecum 3 (Figure 3C) the highest concentration of **8** is formed with 29 μM after 4 h of incubation. For cinnamtannin B1 (**2**) incubated with bacterial suspension of cecum 1 (Figure 3D), **9** and **11** are the main catabolites after 8 h with 33 and 35 μM. Cecum 2 (Figure 3E) mainly catabolized cinnamtannin B1 (**2**) to **10** with a maximum of 50 μM after 8 h of incubation. Cecum 3 (Figure 3F) in contrast produced **8** as the main catabolite after 8 h of incubation with a maximum of 80 μM. The more complicated pattern of hydroxylated catabolites for the degradation of cinnamtannin B1 (**2**) in comparison to procyanidin A2 (**1**) results from the larger and more complex structure of cinnamtannin B1 (**2**). The large interindividual differences between different donor animals concerning the degradation of procyanidins have already been reported earlier for the pig cecum model.[17] With most other models these interindividual differences are not observed due to pooling of the fecal samples, hence losing information about interindividual variations.[24] The interindividual differences make it impossible to characterize an overall trend, but therefore reflect the in vivo situation very well. In humans the gut bacteria are also supposed to metabolize the procyanidins with interindividual differences.

Identification of the Unknown Catabolite of Procyanidin A2 (1). Apart from the already known metabolites, one unknown catabolite was formed for each procyanidin (see FLD-HPLC chromatogram from cecum 1 after incubation with cinnamtannin B1 in the Supporting Information (Figure S3)). Due to the limited amount of the catabolites and the complex matrix accompanying it, no structure elucidation using nuclear

dx.doi.org/10.1021/jf203927g | J. Agric.Food Chem. 2012, 60, 749−757

magnetic resonance spectroscopy could be performed. Therefore, mass spectrometric techniques were used. Using the coupling of HPLC-FLD and FTMS the accurate masses of the catabolites were identified. Detailed FTMS experiments were performed when the signal intensity was sufficient; otherwise, ion trap experiments were performed. FTMS measurements are displayed with the accurate mass; the results of ion trap experiments are given without decimal place due to the unit resolution of the quadrupole instrument. The pseudomolecular ion $[M - H]^-$ of the unknown catabolite **C1** has an accurate mass of m/z 577.1339, which is 2 Da higher than that of the incubated compound A2 (**1**). The proposed formula is $[C_{30}H_{25}O_{12}]^-$, with a calculated m/z of 577.1352, indicating a reduction of procyanidin A2 (**1**). According to the literature the A-type procyanidin procyanidin A2 (**1**) might have been converted into the B-type procyanidin B2 by a reductive cleavage of the C2−C7 ether linkage. This conversion occurs catalyzed by radicals or enzymes.[25,26] Spiking experiments clearly showed that the catabolite **C1** is not procyanidin B2 (data not shown). By comparison of the fragmentation pattern of procyanidin A2 (**1**) and its catabolite, a high similarity can be observed, with most fragments of the catabolite being 2 Da higher except for m/z 285.0404 (calculated for $[C_{15}H_9O_6]^-$ as m/z 285.0405) (Figure 4). To elucidate the structure of the

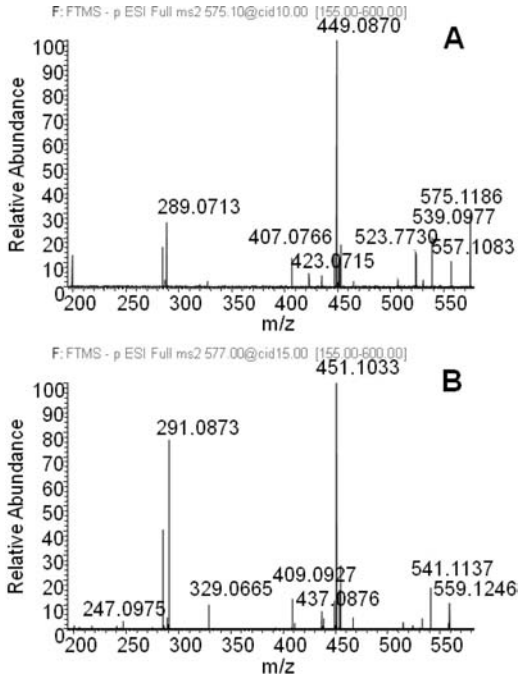

Figure 4. HESI-MS-FTMS product ion spectrum of procyanidin A2 (**1**) (A) and its catabolite **C1** (B) with isolation width of 1.5 and relative fragmentation energy (CID) of 10 V (A) and 15 V (B).

catabolite **C1** we first identified parts of the fragmentation pathway of procyanidin A2 (**1**). In accordance with the literature data, a heterocyclic ring fission (HRF), a retro-Diels-Alder (RDA) fission, and a quinone methide (QM) pathway were identified (Figures 6– 8).[27,28] In contrast to the literature, the typical fragments were measured with exact mass (in the MS fragmentation pathways shown in Figures 6−10 fragments are displayed without decimal places to enhance the clarity of illustration). For procyanidin A2 (**1**) RDA is possible only in the lower unit, which leads to a fragment ion at m/z 423.0715

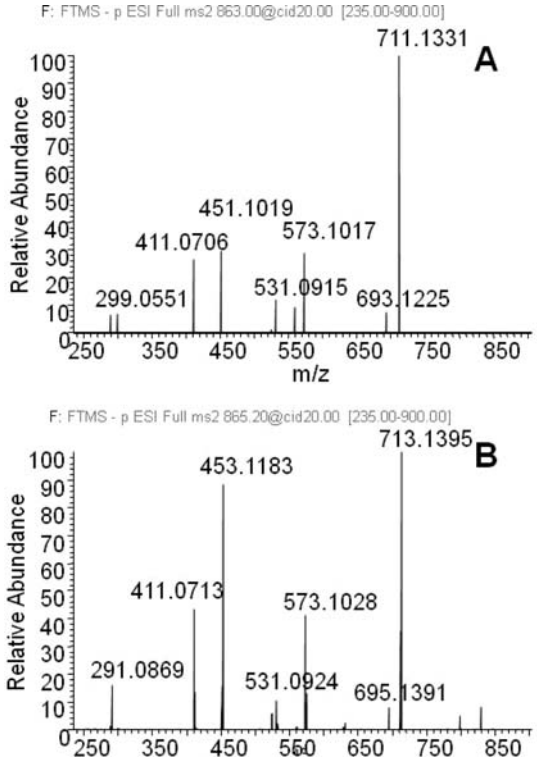

Figure 5. HESI-MS-FTMS product ion spectrum of cinnamtannin B1 (**2**) (A) and its catabolite **C2** (B) with isolation width of 1.5 and relative fragmentation energy (CID) of 20 V.

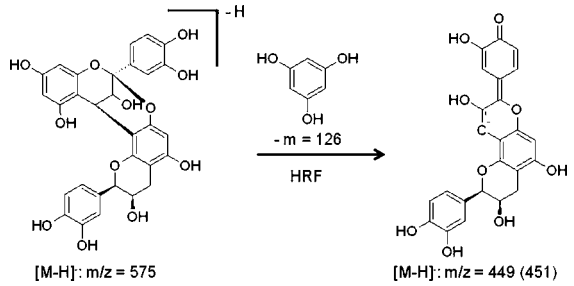

Figure 6. Heterocyclic ring fission (HRF) for procyanidin A2 (**1**).[28] In brackets are the corresponding fragments for the catabolite **C1** (HESI-MS-FTMS).

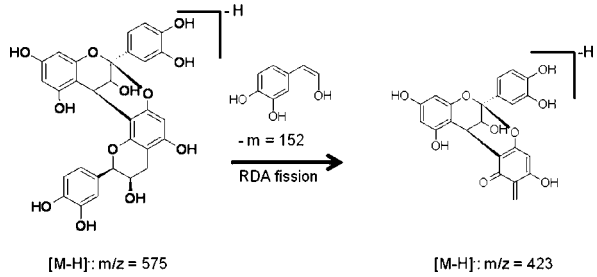

Figure 7. Retro-Diels-Alder (RDA) fission of procyanidin A2 (**1**) (HESI-MS-FTMS).[28] The RDA fission is hindered in catabolite **C1**.

(calculated for $[C_{22}H_{15}O_9]^-$ as m/z 423.0722) (Figure 7).[28] The corresponding fragment at m/z 425 does not exist for the catabolite **C1** (Figure 4), indicating that the RDA fission is hindered. The microbiota therefore caused a change in the C′-ring of the lower monomer moiety in procyanidin A2 (**1**) (for the structure, see Figure 1). The QM pathway of procyanidin

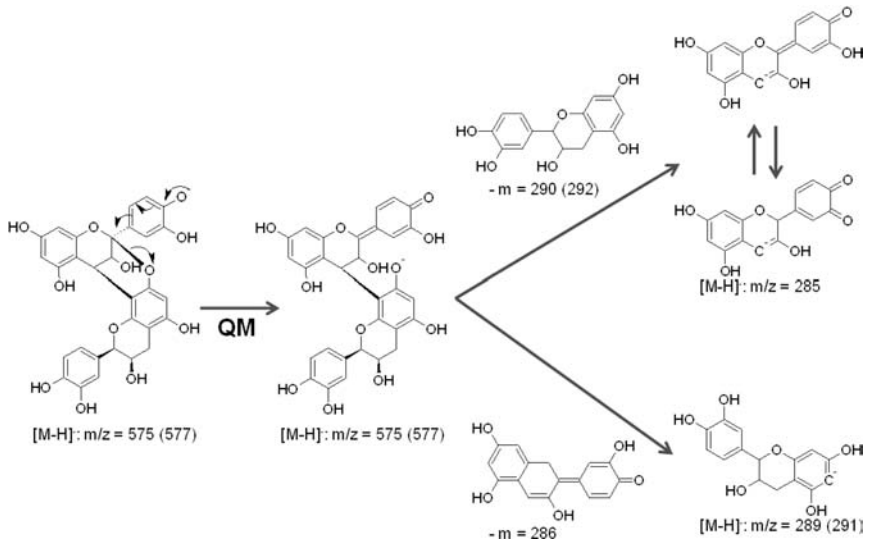

Figure 8. Postulated quinone methide (QM) fragmentation pathway leading to the fragment ions *m/z* 285 and 289 of procyanidin A2 (**1**). In brackets are the corresponding fragments for catabolite **C1** (HESI-MS-FTMS).

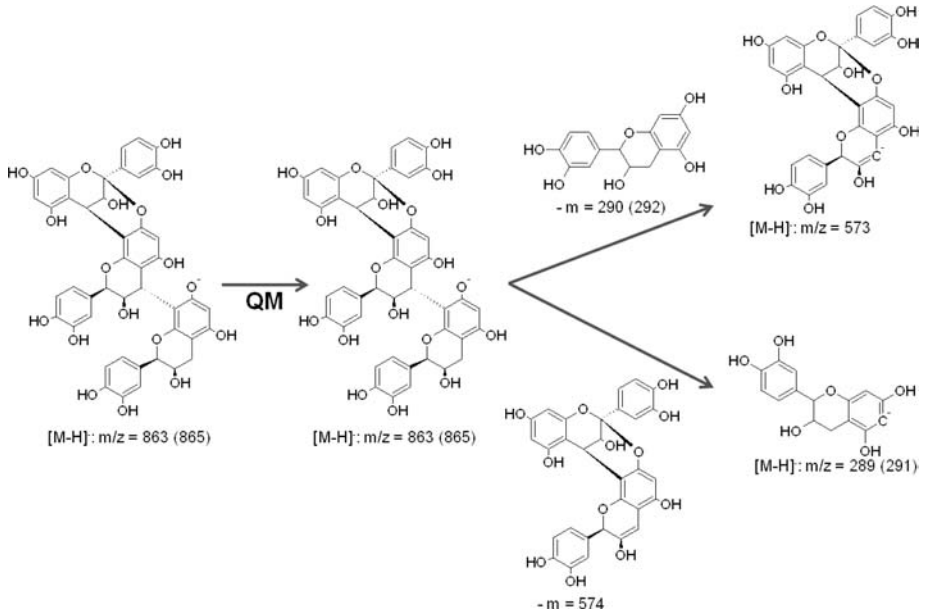

Figure 9. Postulated quinone methide (QM) fragmentation pathway leading to the fragment ions *m/z* 573 and 289 of cinnamtannin B1 (**2**). In brackets are the corresponding fragments for catabolite **C2** (HESI-MS-FTMS).

A2 (**1**) leads to a fragment of *m/z* 289.0713 (calculated for $[C_{15}H_{13}O_6]^-$ as *m/z* 289.0718) of the lower monomer and a fragment of *m/z* 285.0404 (calculated for $[C_{15}H_9O_6]^-$ as *m/z* 285.0405) resulting from the upper monomer (Figure 8).[28] The fragmentation of the catabolite also leads to the fragment of *m/z* 285.0404, but the other fragment for the lower monomer is 2 mass units higher at *m/z* 291.0873 (calculated for $[C_{15}H_{15}O_6]^-$ as *m/z* 291.0874). This also hints that the degradation takes place in the lower unit, leading as expected to a fragment 2 Da higher in comparison to the fragmentation of procyanidin A2 (**1**) for the lower monomer and the same fragment at *m/z* 285 for the upper monomer. The fragmentation pattern for $[M - H]^-$ = 285.0404 from procyanidin A2 (**1**) and its catabolite **C1** in the ion trap were exactly the same (data not shown). Therefore, the RDA fission and the QM pathway of procyanidin A2 (**1**) and its catabolite **C1** clearly showed the degradation to take place at the C′-ring (for the structure, see Figure 1). To find out if a C−C-bond or a C−O-bond of C′ is reduced by the bacteria, the catabolite **C1** was deuterated by exchanging the hydrogen atoms of the hydroxy groups using deuterated methanol/water (50:50). The accurate mass of the catabolite with complete deuterium−hydrogen exchange was $[M - H]^-$ = 586.1910, which leads to a calculated formula of $[C_{30}H_{16}D_9O_{12}]^-$ with *m/z* 586.1916. Therefore, a new hydroxy group is formed. The position of the hydroxy group at the lower monomer was elucidated due to the fact that the fragment $[M - H]^-$ at *m/z* 289 of procyanidin A2 (**1**) as well as $[M - H]^-$ at *m/z* 291 of the catabolite **C1** formed after the QM pathway is able to liberate phloroglucinol (*m/z* 125.0246 calculated for $[C_6H_5O_3]^-$ as *m/z* 125.0244). In conclusion, the catabolite **C1** is formed by the microbiota by cleaving the ether linkage at the C′-ring with the newly formed hydroxy group positioned at the A′-ring (see **C1**, Figure 1). The position of the newly formed hydroxy group at the A-ring is in

dx.doi.org/10.1021/jf203927g | J. Agric.Food Chem. 2012, 60, 749−757

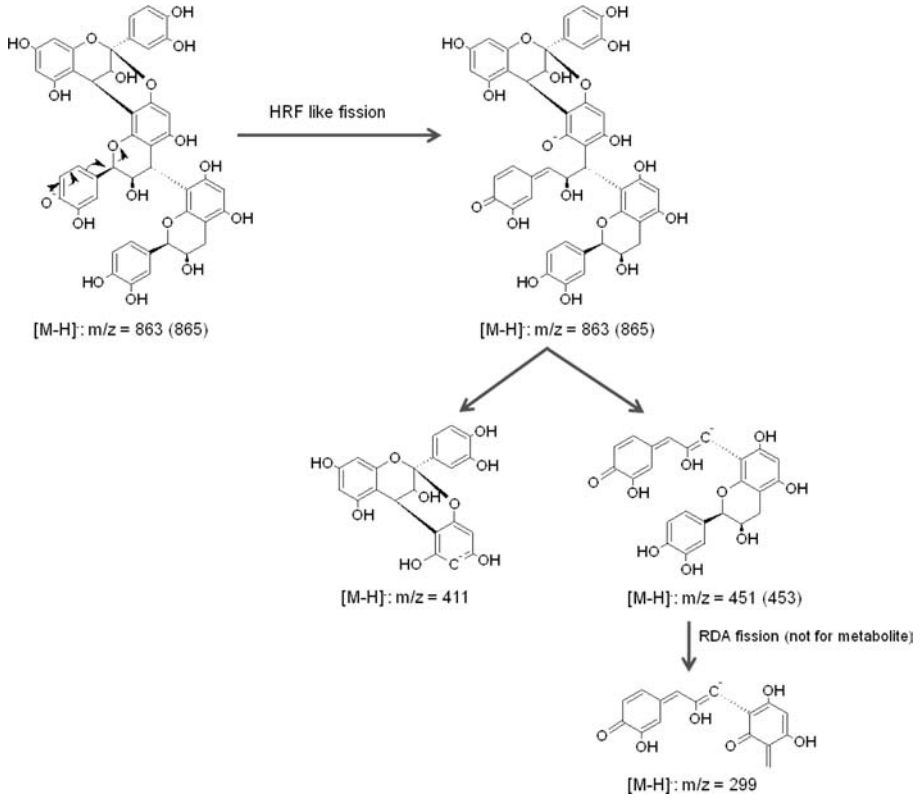

Figure 10. Postulated heterocyclic ring fission (HRF)-like fragmentation pathway leading to the fragment ions *m/z* 411 and 451 of cinnamtannin B1 (**2**). In brackets are the corresponding fragments for catabolite **C2**. Fragment ion *m/z* 451 underlies a retro-Diels-Alder fission to *m/z* 299, which is hindered for catabolite **C2** (HESI-MS-FTMS).

accordance with the literature,[18] where procyanidin B2 was catabolized by porcine microbiota. In contrast to the degradation of a B-type procyanidin dimer, the catabolite of procyanidin A2 (**1**) shows a dimeric character instead of monomeric. After the incubation of procyanidin B2 with human fecal bacteria, catabolites with dimeric and monomeric character could be identified without structural identification of most of the catabolites by LC-MS/MS.[19] Therefore, dimeric catabolites of a B-type procyanidin were already observed but without detailed structure elucidation. To our best knowledge, no studies with microbiota and A-type procyanidins have been performed so far. Due to a missing standard, the formed new catabolite **C1** could not be quantified.

Identification of the Unknown Catabolite of Cinnamtannin B1 (2). After incubation of cinnamtannin B1 (**2**) with porcine microbiota, the formed catabolite **C2** also has an accurate mass 2 Da higher than that of cinnamtannin B1 (**2**) and shows high similarity in regard to the fragmentation pattern of cinnamtannin B1 (**2**), with most of its fragments being 2 Da higher, too (Figure 5). The accurate mass of the pseudomolecular ion $[M - H]^-$ is *m/z* 865.1947 having a calculated formula of $[C_{45}H_{37}O_{18}]^-$ with *m/z* 865.1985. The identification of the fragmentation pathway of cinnamtannin B1 (**2**) is more complex in comparison to the dimer procyanidin A2 (**1**). Several fragments can underlie different fragmentation pathways. For example, RDA fission can take place in the middle or the lower monomeric unit of cinnamtannin B1 (**2**), which in both cases causes the fragment *m/z* 711.1331 (calculated for $[C_{37}H_{27}O_{15}]^-$ as *m/z* 711.1355) for cinnamtannin B1 (**2**) and *m/z* 713.1394 (calculated for $[C_{37}H_{29}O_{15}]^-$ as *m/z* 713.1512) for the catabolite **C2**. From this fragmentation pattern the position of the degradation cannot be identified. The second RDA fission of cinnamtannin B1 (**2**) leads to a fragment of *m/z* 559.0862 (calculated for $[C_{29}H_{19}O_{12}]^-$ as *m/z* 559.0882). A second RDA fission of the catabolite **C2** would induce a fragment of *m/z* 561.0933, which should not occur in analogy to the catabolite of procyanidin A2 (**C1**). However, there is a fragment of *m/z* 561 of the catabolite **C2**, which could be caused by a second RDA fission but can also be explained by a QM pathway with the 2 lower units as residue and an additional loss of water. In addition, the fragment *m/z* 561 of the catabolite bears much less intensity in comparison to the respective fragment of cinnamtannin B1 (**2**), which hints that the fragment results from the QM pathway. From the RDA fission the catabolite hence cannot be further identified. As will be discussed below, the fragments *m/z* 573.1017, 411.0706, 289.0708, and 451.1019 of cinnamtannin B1 (**2**) and *m/z* 573.1027, 411.0713, 291.0868, and 453.1183 of the catabolite **C2** indicated that the intestinal degradation of cinnamtannin B1 (**2**) takes place also at the lowest unit. The fragment *m/z* 573 resulted after a QM pathway with the neutral loss of the lowest unit with a molecular weight of *m* = 290 for cinnamtannin B1 (**2**) and *m* = 292 for the catabolite **C2** (Figure 9). Accordingly, the catabolization happened at the lower monomeric unit of the trimer. This is also supported by the rest of the combined upper and middle monomeric unit of cinnamtannin B1 (**2**) and its catabolite with $[M - H]^-$ at *m/z* 573 showing the same fragmentation pattern (data not shown). The fragment $[M - H]^-$ at *m/z* 291 of the catabolites **C1** and **C2** shows the same fragmentation pattern and similar intensities of the fragments, indicating the same structure. A HRF-like fragmentation can also occur in the middle monomer (Figure 10), resulting in

dx.doi.org/10.1021/jf203927g | J. Agric.Food Chem. 2012, 60, 749–757

fragments with m/z 411 and 451 for cinnamtannin B1 (**2**) and m/z 411 and 453 for the catabolite **C2**, again indicating the alteration occurring in the lowest monomer. Further fragmentation of $[M - H]^-$ at m/z 451 shows a fragment of m/z 299, which occurs after RDA fission. This fragmentation does not appear for $[M - H]^-$ at m/z 453, therefore indicating that the catabolization took place at the C″-ring, resulting in a hindered RDA fission. Analogous to the degradation of procyanidin A2 (**1**) and procyanidin B2, the catabolite **C2** is supposed to have also a new hydroxy group formed, which is positioned at the A″-ring. Thus, we determine the structure of catabolite **C2** as shown in Figure 1. No quantification of this catabolite has been performed in the samples as no standard was available.

Conclusion. To our best knowledge, two yet unknown bacterial procyanidin catabolites were identified by mass spectrometric techniques. LC-FTMS experiments allow the elucidation of unknown procyanidin catabolites. This renders the opportunity for the identification of structures having deficient amount of substance for nuclear magnetic resonance spectroscopy and of catabolites that are embedded in complex matrices. The formed degradation products such as phenolic compounds and the two new catabolites **C1** and **C2** can also be bioavailable and therefore enhance a positive health impact of the procyanidins, which are absorbed to only a low degree during passage through the gastrointestinal tract. It is not certain if the catabolites **C1** and **C2** also bear a potential to cause positive heath impacts. Information concerning the antioxidative potential is lacking. Therefore, an increase or decrease of the antioxidative potential caused by the bacterial catabolism is possible.

■ ASSOCIATED CONTENT

Ⓢ Supporting Information

Detailed concentration profiles of phenolic compounds phloroglucinol, 3,4-dihydroxyphenylbenzoic acid, 4-hydroxyphenylbenzoic acid, 3-hydroxyphenylbenzoic acid, 3-(3,4-dihydroxyphenyl)propionic acid, 3-(4-hydroxyphenyl)-propionic acid, 3(3-hydroxyphenyl)propionic acid, 3,4-dihydroxyphenylacetic acid, 4-hydroxyphenylacetic acid and 3-hydroxyphenylacetic acid (**3**−**12**) as degradation products of procyanidin A2 (**1**) and cinnamtannin B1 (**2**) for three different ceca are shown in Figure S1 and Figure S2, respectively; a HPLC−fluorescence chromatogram of the feces extract after incubation of cecum 1 with 100 μM cinnamtannin B1 after 20 min and 8 h of incubation time is shown in Figure S3. This material is available free of charge via the Internet at http://pubs.acs.org.

■ AUTHOR INFORMATION

Corresponding Author

*Phone: +49 251 8333391. Fax: +49 251 8333396. E-mail: humpf@uni-muenster.de.

Funding

Financial support from the NRW Graduate School of Chemistry is gratefully acknowledged.

■ ACKNOWLEDGMENTS

We thank the Kurzen family (Gut Wewel, Senden, Germany) for providing the ceca.

■ ABBREVIATIONS USED

BSA, *N*,*O*-bis(trimethylsilyl)acetamide; CB1, cinnamtannin B1; CID, collision-induced dissociation; DAD, diode array detector; 3,4-DHAA, 3,4-dihydroxyphenylacetic acid; 3,4-DHBA, 3,4-dihydroxyphenylbenzoic acid; 3-(3,4-DH)PA, 3-(3,4-dihydroxyphenyl)propionic acid; EI, electron impact ionization; ESI, electrospray ionization; FLD, fluorescence detector/detection; FTMS, Fourier transform mass spectrometry; GC, gas chromatography; HCl, hydrochloric acid; HESI, heated electrospray ionization; 3-HAA, 3-hydroxyphenylacetic acid; 4-HAA, 4-hydroxyphenylacetic acid; 3-HBA, 3-hydroxyphenylbenzoic acid; 4-HBA, 4-hydroxyphenylbenzoic acid; 3-(3-H)PA, 3-(3-hydroxyphenyl)propionic acid; 3-(4-H)PA, 3-(4-hydroxyphenyl)propionic acid; HPLC, high-performance liquid chromatography; HRF, heterocyclic ring fission; LC-FTMS, liquid chromatography coupled with Fourier transform mass spectrometry; PA2, procyanidin A2; QM, quinone methide; RDA, retro-Diels-Alder.

■ REFERENCES

(1) Williamson, G.; Manach, C. Bioavailability and bioefficacy of polyphenols in humans. II. Review of 93 intervention studies. *Am. J. Clin. Nutr.* **2005**, *81* (1 Suppl.), 243S−255S.

(2) da Silva Porto, P. A.; Laranjinha, J. A.; de Freitas, V. A. Antioxidant protection of low density lipoprotein by procyanidins: structure/activity relationships. *Biochem. Pharmacol.* **2003**, *66* (6), 947−954.

(3) Miura, T.; Chiba, M.; Kasai, K.; Nozaka, H.; Nakamura, T.; Shoji, T.; Kanda, T.; Ohtake, Y.; Sato, T. Apple procyanidins induce tumor cell apoptosis through mitochondrial pathway activation of caspase-3. *Carcinogenesis* **2008**, *29* (3), 585−593.

(4) Lopez, J. J.; Jardin, I.; Salido, G. M.; Rosado, J. A. Cinnamtannin B-1 as an antioxidant and platelet aggregation inhibitor. *Life Sci* **2008**, *82* (19−20), 977−982.

(5) Rasmussen, S. E.; Frederiksen, H.; Krogholm, K. S.; Poulsen, L. Dietary proanthocyanidins: occurrence, dietary intake, bioavailability, and protection against cardiovascular disease. *Mol. Nutr. Food Res.* **2005**, *49*, 159−174.

(6) Rzeppa, S.; von Bargen, C.; Bittner, K.; Humpf, H. U. Analysis of flavan-3-ols and procyanidins in food samples by reversed phase high-performance liquid chromatography coupled to electrospray ionization tandem mass spectrometry (RP-HPLC-ESI-MS/MS). *J. Agric. Food Chem.* **2011**, *59* (19), 10594−10603.

(7) Serra, A.; Macia, A.; Romero, M. P.; Valls, J.; Blade, C.; Arola, L.; Motilva, M. J. Bioavailability of procyanidin dimers and trimers and matrix food effects in in vitro and in vivo models. *Br. J. Nutr.* **2009**, *103* (7), 944−952.

(8) Rios, L. Y.; Bennett, R. N.; Lazarus, S. A.; Remesy, C.; Scalbert, A.; Williamson, G. Cocoa procyanidins are stable during gastric transit in humans. *Am. J. Clin. Nutr.* **2002**, *76* (5), 1106−1110.

(9) Kahle, K.; Kempf, M.; Schreier, P.; Scheppach, W.; Schrenk, D.; Kautenburger, T.; Hecker, D.; Huemmer, W.; Ackermann, M.; Richling, E. Intestinal transit and systematic metabolism of apple polyphenols. *Eur. J. Nutr.* **2011**, *50*, 507−522.

(10) Appeldoorn, M. M.; Vincken, J. P.; Gruppen, H.; Hollman, P. C. Procyanidin dimers A1, A2, and B2 are absorbed without conjugation or methylation from the small intestine of rats. *J. Nutr.* **2009**, *139* (8), 1469−1473.

(11) Manach, C.; Scalbert, A.; Morand, C.; Remesy, C.; Jimenez, L. Polyphenols: food sources and bioavailability. *Am. J. Clin. Nutr.* **2004**, *79* (5), 727−747.

(12) Seefelder, W. *Fumonisine und deren Reaktionsprodukte: Vorkommen, Bedeutung, biologische Aktivität und Metabolsimus*; Würzburg, Bayrische Julius-Maximilian-Universität, Institut für Lebensmittelchemie: Würzburg, Germany, 2002.

(13) Hein, E. M.; Rose, K.; van't Slot, G.; Friedrich, A. W.; Humpf, H. U. Deconjugation and degradation of flavonol glycosides by pig

cecal microbiota characterized by fluorescence in situ hybridization (FISH). *J. Agric. Food Chem.* **2008**, *56* (6), 2281−2290.
(14) Keppler, K.; Humpf, H.-U. Metabolism of anthocyanins and their phenolic degradation products by the intestinal microflora. *Bioorg. Med. Chem.* **2005**, *13* (17), 5195−5205.
(15) Wang, L.-Q.; Meselhy, M. R.; Li, Y.; Nakamura, N.; Min, B.-S.; Qin, G.-W.; Hattori, M. The heterocyclic ring fission and dehydroxylation of catechins and related compounds by *Eubacterium* sp. strain SDG-2, a human intestinal bacterium. *Chem. Pharm. Bull.* **2001**, *49* (12), 1640−1643.
(16) Keppler, K.; Hein, E. M.; Humpf, H.-U. Metabolism of quercetin and rutin by the pig caecal microflora prepared by freeze-preservation. *Mol. Nutr. Food Res.* **2006**, *50* (8), 686−695.
(17) van't Slot, G.; Humpf, H. U. Degradation and metabolism of catechin, epigallocatechin-3-gallate (EGCG), and related compounds by the intestinal microbiota in the pig cecum model. *J. Agric. Food Chem.* **2009**, *57* (17), 8041−8048.
(18) van't Slot, G.; Mattern, W.; Rzeppa, S.; Grewe, D.; Humpf, H. U. Complex flavonoids in cocoa: synthesis and degradation by intestinal microbiota. *J. Agric. Food Chem.* **2010**, *58* (15), 8879−8886.
(19) Stoupi, S.; Williamson, G.; Drynan, J. W.; Barron, D.; Clifford, M. N. Procyanidin B2 catabolism by human fecal microflora: partial characterization of 'dimeric' intermediates. *Arch. Biochem. Biophys.* **2010**, *501* (1), 73−78.
(20) Liu, L.; Xie, B.; Cao, S.; Yang, E.; Xu, X.; Guo, S. A-type procyanidins from Litchi chinensis pericarp with antioxidant activity. *Food Chem.* **2007**, *105*, 1446−1451.
(21) Virtbauer, J.; Krenn, L.; Kahlig, H.; Hufner, A.; Donath, O.; Marian, B. Chemical and pharmacological investigations of *Metaxya rostrata*. *Z. Naturforsch. C* **2008**, *63* (7−8), 469−475.
(22) Jayaprakasha, G. K.; Ohnishi-Kameyama, M.; Ono, H.; Yoshida, M.; Jaganmohan Rao, L. Phenolic constituents in the fruits of *Cinnamomum zeylanicum* and their antioxidant activity. *J. Agric. Food Chem.* **2006**, *54* (5), 1672−1679.
(23) Kamiya, K.; Watanabe, C.; Endang, H.; Umar, M.; Satake, T. Studies on the constituents of bark of *Parameria laevigata* Moldenke. *Chem. Pharm. Bull. (Tokyo)* **2001**, *49* (5), 551−557.
(24) Appeldoorn, M. M.; Vincken, J. P.; Aura, A. M.; Hollman, P. C.; Gruppen, H. Procyanidin dimers are metabolized by human microbiota with 2-(3,4-dihydroxyphenyl)acetic acid and 5-(3,4-dihydroxyphenyl)-γ-valerolactone as the major metabolites. *J. Agric. Food Chem.* **2009**, *57* (3), 1084−1092.
(25) Kondo, K.; Kurihara, M.; Fukuhara, K.; Tanaka, T.; Suzuki, T.; Miyata, N.; Toyoda, M. Conversion of procyanidin B-type (catechin dimer) to A-type: evidence for abstraction of C-2 hydrogen in catechin during radical oxidation. *Tetrahedron Lett.* **2000**, *41*, 485−488.
(26) Osman, A. M.; Wong, K. K. Y. Laccase (EC 1.10.3.2) catalyses the conversion of procyanidin B-2 (epicatechin dimer) to type A-2. *Tetrahedron Lett.* **2007**, *48*, 1163−1167.
(27) Friedrich, W.; Eberhardt, A.; Galensa, R. Investigation of proanthocyanidins by HPLC with electrospray ionization mass spectrometry. *Eur. Food Res. Technol.* **1999**, *211*, 56−64.
(28) Karchesy, J. J.; Foo, L. Y.; Barofsky, E.; Arbogast, B.; Barofsky, D. F. Negative-ion fast-atom-bombardment mass spectrometry of procyanidin oligomers. *J. Wood Chem. Technol.* **1989**, *9* (3), 313−331.